

# The two sides of a lipid-protein story

Luis G. Mansor Basso<sup>1</sup> · Luis F. Santos Mendes<sup>1</sup> · Antonio J. Costa-Filho<sup>1</sup>

Received: 13 March 2016 / Accepted: 29 March 2016 / Published online: 30 April 2016

© International Union for Pure and Applied Biophysics (IUPAB) and Springer-Verlag Berlin Heidelberg 2016

**Abstract** Protein–membrane interactions play essential roles in a variety of cell functions such as signaling, membrane trafficking, and transport. Membrane-recruited cytosolic proteins that interact transiently and interfacially with lipid bilayers perform several of those functions. Experimental techniques capable of probing changes on the structural dynamics of this weak association are surprisingly limited. Among such techniques, electron spin resonance (ESR) has the enormous advantage of providing valuable local information from both membrane and protein perspectives by using intrinsic paramagnetic probes in metalloproteins or by attaching nitroxide spin labels to proteins and lipids. In this review, we discuss the power of ESR to unravel relevant structural and functional details of lipid–peripheral membrane protein interactions with special emphasis on local changes of specific regions of the protein and/or the lipids. First, we show how ESR can be used to investigate the direct interaction between a protein and a particular lipid, illustrating the case of lipid binding into a hydrophobic pocket of chlorocatechol 1,2-dioxygenase, a non-heme iron enzyme responsible for catabolism of aromatic compounds that are industrially released in the environment. In the second case, we show the effects of GPI-anchored tissue-nonspecific alkaline phosphatase, a protein that plays a crucial role in skeletal mineralization, and on the ordering and dynamics of lipid acyl chains. Then, switching to the protein perspective, we analyze the interaction with model

membranes of the brain fatty acid binding protein, the major actor in the reversible binding and transport of hydrophobic ligands such as long-chain, saturated, or unsaturated fatty acids. Finally, we conclude by discussing how both lipid and protein views can be associated to address a common question regarding the molecular mechanism by which dihydroorotate dehydrogenase, an essential enzyme for the de novo synthesis of pyrimidine nucleotides, and how it fishes out membrane-embedded quinones to perform its function.

**Keywords** Protein–lipid interaction · Protein–membrane interaction · ESR · EPR · Spin labeling · Metalloproteins

## Introduction

A major event in life origin and evolution concerns the ability of the cell membrane to separate its cytoplasm from the extracellular environment. This wall, or plasma membrane, is of paramount importance for the enclosure of all compounds necessary for cell maintenance as well as for functioning as a selective barrier for the diffusion of a variety of ions, biomolecules, gases, etc. In the cell membrane, membrane-attached, or membrane-embedded proteins perform many different functions, such as transport, signaling, and membrane fusion (Cho and Stahelin 2005; Goñi 2002; Alberts et al. 2007).

It is estimated that 30–40% of all cell proteins are membrane-associated proteins, clearly showing the relevance of this protein class to cell function (Arora and Tamm 2001; Smith et al. 2001). Moreover, it is believed that more than 50% of all present and future drug targets involve membrane-associated proteins (Hemminga 2007). Within the membrane protein class, transiently-associated proteins interact through mechanisms based either on a dynamic

Luis G. Mansor Basso and Luis F. Santos Mendes contributed equally to this work.

✉ Antonio J. Costa-Filho  
ajcosta@ffclrp.usp.br

<sup>1</sup> Laboratório de Biofísica Molecular, Departamento de Física, Faculdade de Filosofia, Ciências e Letras de Ribeirão Preto, Universidade de São Paulo, Ribeirão Preto, SP, Brazil

equilibrium (surface interaction) or on a post-translation modification, such as GPI-, palmitoyl- or myristoyl-anchor. These so-called peripheral membrane proteins are related to important biological functions, such as kinases (Hurley 2006), regulatory subunits of ion channels and transmembrane receptors (Stott et al. 2015), hormones (Vauquelin and Packeu 2009),  $\text{Ca}^{2+}$  homeostasis and inflammatory response (Garcia et al. 2013), antimicrobial factors (Vicente et al. 2013), and others (Alberts et al. 2007). Information on transient interactions can be challenging to obtain but, fortunately, experimental techniques are available that address issues such as circular dichroism (CD) (Matsuo et al. 2016), static and time-resolved fluorescence (Munishkina and Fink 2007; Johnson 2005), the Langmuir monolayer technique (Brockman 1999; Dua et al. 2005), calorimetry (Situ et al. 2014; Cañadas and Casals 2013), and nuclear (Franks et al. 2012; Judge et al. 2015) and electron (Páli and Kóta 2013; Hubbell et al. 2013) magnetic resonances, among others (Saliba et al. 2015; Tatulian 2013; Kleinschmidt 2013).

Each of these techniques has deficiencies. CD is capable of monitoring protein structural transitions upon membrane interaction, but is blind to interactions without structural rearrangements and does not provide local structural information. Fluorescence techniques have the advantage of their high sensitivity, but the use of bulky fluorescent labels might disturb the protein structure. The Langmuir monolayer provides an excellent model of a two-dimensional ordered system at very little expense, but depending on the biophysical information needed it may not provide a sufficiently representative model for a biological membrane. Differential scanning calorimetry and isothermal titration calorimetry are the most powerful techniques available to unravel the thermodynamics of binding and can be used to monitor both membrane and protein structural integrity and binding mechanisms in different environments. However, calorimetric methods require large amounts of samples and, like CD, cannot provide local information. Nuclear magnetic resonance (NMR) provides atomic-resolution structural and dynamics data of both proteins and membranes, but has the limitation of isotopic labeling, molecular mass, high sample concentration, and the difficult task related to data analysis for a general user. Electron magnetic resonance, or electron spin resonance (ESR), is a powerful tool to study protein–membrane interactions and provides information from both perspectives: the “membrane side”, by using spin-labeled lipids, and the “protein side”, by using the so-called site-directed spin labeling (SDSL) technique (Hubbell and Altenbach 1994). Specifically, in the case of protein–lipid interactions, continuous wave (CW) ESR can be applied, for instance to quantify physicochemical disturbance of membrane model systems upon protein interaction and to detect protein domains that are responsible for membrane binding and/or anchoring and their accompanying dynamical changes. Furthermore, the high sensitivity of ESR has

the advantage of low level (nM to  $\mu\text{M}$  range) labeled molecules and very few limitations on buffer composition or sample size. This review focuses on representative data from our laboratory to enlighten the power of the spin labeling CW-ESR spectroscopy applied to studies of protein–lipid interactions, with special emphasis on peripheral membrane proteins.

### Spin labeling electron spin resonance (ESR)

Like NMR spectroscopy, ESR monitors the resonant energy absorption from a radiation field when magnetic-active molecules change their energy states. If the molecule possesses an unpaired electron, its magnetic dipole interacts with the magnetic component of the radiation field, thus allowing energy transfer. However, since the energy levels corresponding to different spin states coincide, no transition occurs unless a strong external magnetic field is applied. This Zeeman interaction splits the energy states, therefore allowing the observation of the transition between them provided that the energy of the oscillating magnetic field, occurring at microwave frequencies, matches the energy difference between the spin states. This is the physical basis of the ESR spectroscopy (Guzzi and Bartucci 2015; Fajer 2000). The simplest ESR example is an unpaired electron in a molecular orbital, whose spectrum will correspond to just one Lorentzian resonant line.

The application of ESR in studies of biomacromolecules has been limited in the past to just a subclass of metalloproteins, i.e. proteins bearing naturally occurring ESR-active metal centers such as iron, copper, manganese, cobalt, and molybdenum (Hanson and Berliner 2009). With the advent of spin-labeling techniques and improvements in chemical synthesis methodologies, ESR has been extended to the diamagnetic world. Hence, previously ESR-silent proteins, lipids, and nucleic acids involved in a variety of cell functions can be investigated by spin labeling ESR (Berliner and Reuben 1989; Sowa and Qin 2008). In the specific case of studies of protein–lipid interactions, both can be spin labeled so that biologically important mechanistic and functional ‘stories’ can be accounted for by reports from both lipid and protein perspectives.

The most commonly used spin labels in biological systems are based on the nitroxide (NO) radical (Fajer 2000). Nitroxide compounds possess an unpaired electron ( $S = 1/2$ ) in the N–O bond and a non-zero nuclear spin ( $I = 1$ ) in the nitrogen nucleus that interacts with the unpaired electron via a dipole–dipole coupling called hyperfine interaction. This interaction gives rise to a multiplet structure corresponding to three resonant lines. Once covalently attached to the biomolecule of interest, these spin probes provide important structural and dynamic information on their surroundings. Nitroxide-labeled fatty acids and phospholipids (such as 16-PCSL; Fig. 1) can be obtained both commercially by laboratory-

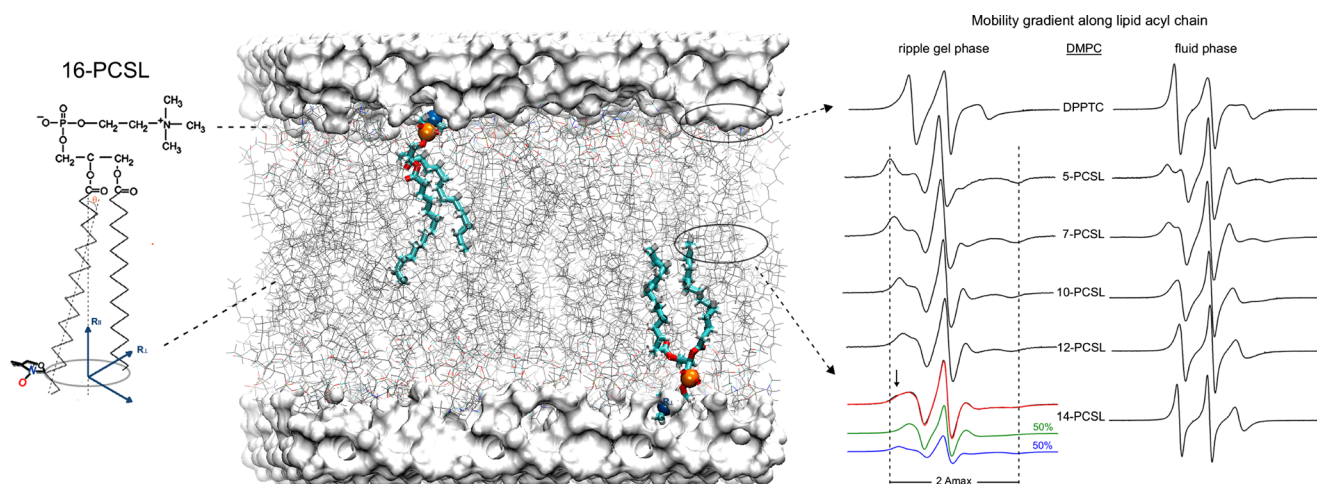


**Fig. 1** Spin labeling ESR from the membrane perspective and structural dynamics-line-shape correlations. **a** Dimiristoylphosphatidylcholine (DMPC) lipid bilayer (stick representation in gray) usually doped with 0.5–1.0 mol% of spin-labeled lipids containing a nitroxide radical attached to different positions along the lipid acyl chain, such as the spin label 16-PCSL on the left. A particular phospholipid is highlighted in licorice representation with the phosphorus and nitrogen atoms of the lipid head group colored in orange and blue, respectively. Different n-PCSL ( $n = 5, 7, 10, 12, 14$ , and 16) spin labels report on specific regions of the lipid bilayer. On the right, typical n-PCSL ESR spectra obtained for DMPC in the ripple gel phase (20 °C) and in fluid phase (35 °C). It is

worth noting the lineshape changes of the spectra due to the mobility gradient experienced by the spin labels from the head group region down to the hydrophobic core of the lipid bilayer and also the lipid phase-dependence of the lineshape. Coexistence of two spin populations presenting different ordering and dynamics can also be detected by ESR, as shown by the 14-PCSL in the DMPC ripple gel phase. The lipid bilayer was built with CHARMM-GUI Membrane Builder (<http://www.charmm-gui.org/input/membrane>) (Jo et al. 2008; Wu et al. 2014) and rendered with Visual Molecular Dynamics (Humphrey et al. 1996). Adapted from (Basso et al. 2011) with permission

based chemical synthesis (Marsh and Watts 1982; Wolfs et al. 1989) and are able to monitor distinct regions of model and biological membranes (Fig. 1). On the other hand, proteins can be spin labeled by using site-directed spin labeling (SDSL) (Hubbell and Altenbach 1994). In this approach, mutagenesis is used to replace a native amino acid residue at a desired site for a cysteine followed by a reaction with a nitroxide reagent such as methanethiosulfonate spin label (MTSL), the most frequent label used for proteins (Hubbell and Altenbach 1994). The resulting paramagnetic side chain is often called R1 (Fig. 2a). MTSL-non-reactive residues like serines or alanines can replace additional cysteines in the protein structure. Each mutant produced needs to be tested for protein function and folding, and those inactive or unfolded are discarded. MTSL-labeling can be achieved at virtually any secondary structural element with reasonable solvent accessibility (Mchaourab et al. 1996; Hubbell et al. 1998).

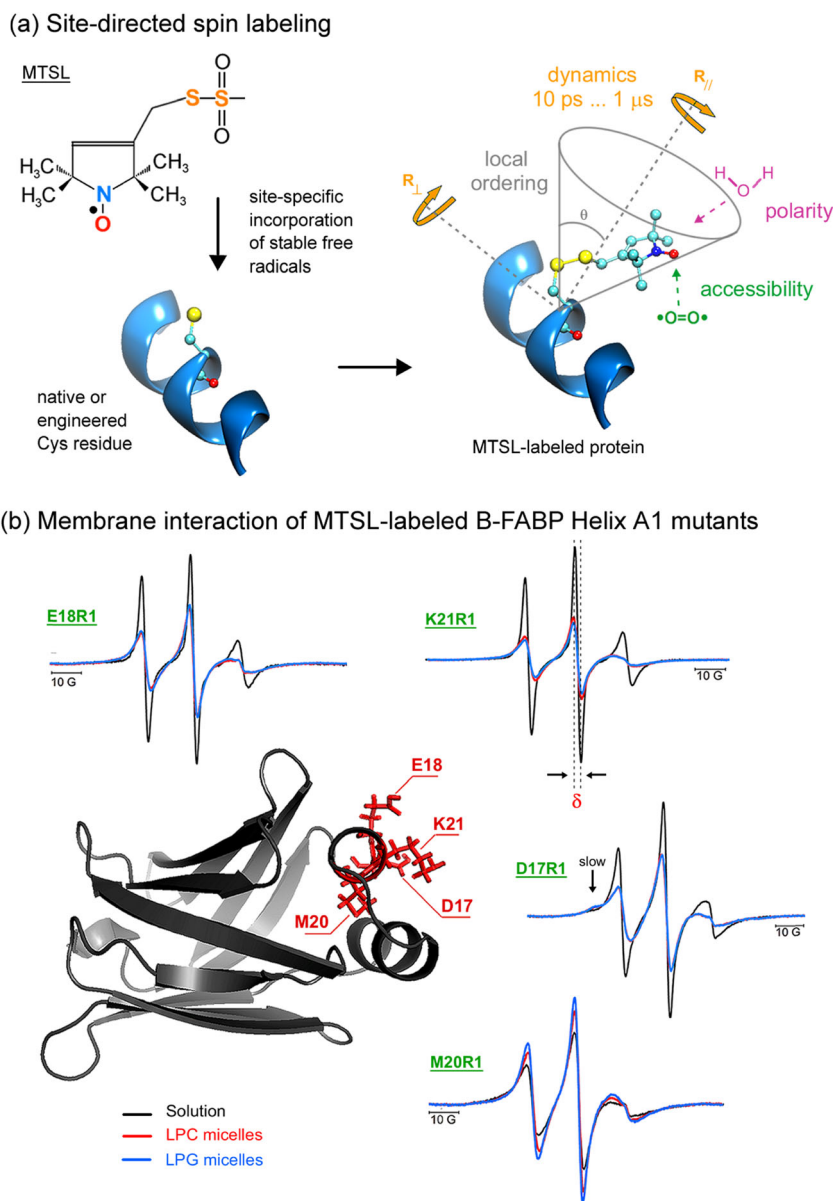
ESR spectra from spin-labeled molecules generally report on local ordering, mobility, accessibility to polar and non-polar paramagnetic compounds, and on the polarity and proticity (ability to donate a hydrogen bond) of the surrounding microenvironment of the spin label. All that information might be relevant to unravel complex biological mechanisms that take place during protein–lipid interactions. When embedded into model or biological membranes, spin-labeled lipids also provide insights into membrane fluidity, phase state, coexistence of different lipid microdomains in membranes, or even the coexistence of bulk and boundary

(protein-bound) lipids in protein–membrane systems, among others (Swamy et al. 2006; Altenbach et al. 1994; Marsh 2001; Costa-Filho et al. 2003; Marsh et al. 1982; Barroso et al. 2015). On the other hand, ESR spectra of MTSL-labeled proteins can be used to detect changes in protein conformation, backbone dynamics, tertiary interactions, and secondary structure (Hubbell et al. 2000; Langen et al. 2000; Columbus and Hubbell 2002), and to accurately measure intra- and inter-molecular distances between the paramagnetic probes in doubly- or singly-labeled proteins, respectively, on a nanometer length scale by using CW (0.5–2.5 nm) or pulsed (1.5–8.0 nm) ESR techniques (Jeschke 2012; Jeschke and Polyhach 2007; Borbat and Freed 1999; Berliner et al. 2000).

Lipids and proteins are inherently dynamic molecules whose local and collective motions have long been recognized to modulate their function (Marsh 2008). In this context, the spin label orientation can be significantly affected by the molecular dynamics of the protein and/or the lipid, giving rise to line shape changes due to the modulation of the anisotropic Zeeman ( $g$ -tensor) and hyperfine interactions. The faster the motion, the more averaged are the interactions. Conventional CW-ESR spectrum at the X band (9 GHz) is sensitive to motions whose rotational correlation times ( $\tau_R$ ) are in the range of  $10^{-11}$ – $10^{-7}$  s and are primarily determined by the transverse spin–spin relaxation time,  $T_2$  (Fajer 2000; Berliner and Reuben 1989). At this frequency, three distinct motional regimes are defined. In the fast motion regime, where  $10^{-11} < \tau_R < 10^{-9}$  s,  $g$ -tensor and hyperfine splitting are averaged and the

**Fig. 2** Spin labeling ESR from the protein perspective. **a**

Attachment of methanethiosulfonate spin label (MTSL) to a native or an engineered cysteine residue give rise to the side chain designated as R1 of the spin-labeled protein. ESR can provide valuable local information of the probe vicinity. See text for more details. **b** Sites of introduction of single R1 residues, one at a time, in the  $\alpha$ -helix A1 of the native structure of human B-FABP (PDB ID: 1JJX) along with the corresponding ESR spectra of the mutants D17R1, E18R1, M20R1, and K21R1 in the membrane-bound (lysophosphatidylcholine – LPC – red; lysophosphatidylglycerol – LPG – blue) and solution (black) states. The arrow in the D17R1 spectrum denotes the more immobilized, ordered spin population that appeared in the presence of the micelles. ESR spectra, acquired at room temperature and with a scan range of 100 G, were normalized to the number of spins to facilitate the analysis: the less intense the spectrum, the more broadened it is, which means a more packed or less mobile spin label. Arrows point to a second, more ordered component in the ESR spectra of D17R1 and G33R1.  $\delta$  corresponds to the central linewidth, whose inverse value is proportional to the mobility. Adapted from Dyszy et al. (2013) with permission



sensitivity of the spectrum to changes in  $\tau_R$  is high. The resulting ESR spectrum presents a typical three narrow lines pattern such as those observed for 16-PCSL in the dimyristoylphosphatidylcholine (DMPC) fluid phase (Fig. 1). In this regime,  $\tau_R$  and order parameters can be calculated from empirical parameters defined over the spectrum (Fajer 2000) using Redfield's perturbation theory (Redfield 1965). In the slow motion regime, where  $10^{-9} \text{ s} < \tau_R < 2 \times 10^{-7} \text{ s}$ , the spectrum still provides good sensitivity, but Redfield's theory does not hold. Instead, non-linear least-squares (NLLS) spectral simulations based on the stochastic Liouville equation have been used to obtain quantitative information, such as rotational diffusion rates and order parameters (Schneider and Freed 1989; Budil et al. 1996). The line shape is usually broader than the ones from the faster motional

regime, for example the 5-PCSL spectrum in the DMPC ripple gel phase (Fig. 1). In the rigid motion regime, where  $\tau_R > 2 \times 10^{-7} \text{ s}$ , the conventional 9-GHz CW ESR line shape presents the poorest sensitivity to motion, since the rotational mobility of the spin label is too slow compared to the X-band ESR timescale, thus no longer affecting hyperfine or g-tensor anisotropy. Typical ESR spectra in this motional regime are much broader than the previously mentioned ones. This is mostly because very slow motions affect the longitudinal magnetization much more, which decays with the spin–lattice relaxation time,  $T_1$ , instead of the transverse magnetization, which decays with  $T_2$ . The development of other CW and pulsed ESR techniques that take advantage of  $T_1$  along with multifrequency ESR have extended the range of the ESR timescale from  $10^{-12}$  to  $\sim 10^{-4} \text{ s}$ , which virtually covered up

a broad range of local and collective molecular motions of proteins and membranes and have greatly contributed to the success of ESR in protein–membrane studies (Borbat et al. 2001; Jeschke et al. 2004; McHaourab et al. 2011; Sahu and Lorigan 2015; Smirnova and Smirnov 2015).

The motional-dependence of the conventional X-band CW ESR line shape can be easily visualized by considering the spin-labeled lipids of Fig. 1 embedded in a DMPC lipid bilayer. Nitroxide radicals attached to different positions of the lipid acyl chain and the head group region give rise to very distinct ESR line shapes. The isotropic-like, motionally-averaged 14-PCSL ESR spectrum in the fluid phase becomes broader as the nitroxide is moved from the 14th up to the 5th carbon position (5-PCSL). This mobility gradient reflects the increased fluidity gradient usually observed toward the center of the lipid bilayer (Hubbell and McConnell 1969; Hubbell and McConnell 1971; Seelig and Hasselbach 1971). The corresponding gel-phase n-PCSL signals are considerably broader than the fluid-phase ones, thus reflecting more ordered and less mobile gel-phase lipids. Due to its higher sensitivity to motions, 14-PCSL is able to report on the coexistence of fluid-like and gel-like micro-domains in the DMPC ripple gel phase. A ‘shoulder’ in the low-field line of the 14-PCSL spectrum appears (arrow in Fig. 1), indicating a typical two-component ESR signal with distinct ordering and dynamics. NLLS simulations provided order parameters, rotational diffusion rates and percentage of populations of the spin-labeled lipids partitioned in both microdomains (Basso et al. 2011). Due to the strong ionic interactions between the lipid head groups, primarily generated by hydrogen bonding, ESR spectra of the head-group spin-labeled DPPTC reflect a highly ordered region with restricted mobility (Ge and Freed 2009). The difference in its line shape compared to the n-PCSL is primarily due to the dependence of the head-group orientation on the lipid phase state that tends to align the nitroxide radical perpendicular or parallel to the bilayer surface as revealed by NLLS simulations (Ge and Freed 1998). This qualitative description of the ESR spectra of nitroxide-labeled lipids embedded in membranes also holds true for the motional-dependence of the line shape of spin-labeled proteins.

Generally speaking, the broader the line-shape of a spin-normalized spectrum, the slower the motion. Thus, the inverse of the width of the central resonance line,  $\delta^{-1}$ , is a good indicator of mobility (Hubbell et al. 2000) and can thus be used to extract qualitative information about changes in dynamics due to protein–lipid interactions. For instance, the ESR spectra of the MTSL-labeled protein illustrated in Fig. 2b show less (more) intense signals for some residues, i.e., more (less) broadened spectra upon membrane binding compared to their spectra in solution, suggesting a more (less) immobilized residue upon membrane interaction.

In the subsequent sections, we illustrate with a few examples of how line-shape alterations of the conventional CW-

ESR spectra can be translated into lipid or protein conformational changes, and how that information can be used to infer the protein function or mechanism of action.

### Case 1. Chlorocatechol 1,2-dioxygenase (CCD)

The biotechnological use of microorganisms has emerged as an excellent approach against the accumulation of industrial polycyclic hydrocarbons pollution (Ornston and Stanier 1966). Oxidation of cyclic hydrocarbons performed by bacteria genera, especially *Pseudomonas putida*, relies on the dioxygenase family of non-heme iron proteins (Atlas and Cerniglia 1995). These proteins play a special role in the metabolic funnel for degradation of cyclic hydrocarbons compounds, with catechol (or its derivatives) being the common intermediate (Bugg and Ramaswamy 2008). Chlorocatechol 1,2-dioxygenase (1,2-CCD) from *P. putida*, a dioxygenase family member, has been extensively studied with respect to its structure, function, and biological regulation (Citadini et al. 2005; Mesquita et al. 2013; Solomon et al. 2000).

1,2-CCD is a soluble protein that makes use of a hydrophobic channel in the dimerization interface to bind amphipathic molecules, such as phospholipids, that regulate its kinetics profile (Citadini et al. 2005; Mesquita et al. 2013; Vetting and Ohlendorf 2000; Ferraroni et al. 2004). Citadini et al. (2005) described this isolated lipid–protein binding from the lipid perspective by using spin-labeled stearic acids and phospholipids as paramagnetic probes for ESR. They observed a particular spectral pattern for all probes that shows a coexistence of two different populations: one more restricted, representing 1,2-CCD-bound lipids, and the other more mobile, representing free lipids in solution. The authors also noticed a ‘V-shape’ mobility profile for all the probes in the protein hydrophobic tunnel: the rotational diffusion rate decreased, for instance, from  $2.0 \times 10^7 \text{ s}^{-1}$  for 5-PCSL down to  $0.6 \times 10^7 \text{ s}^{-1}$  for 10-PCSL and increased 3-fold again to  $1.8 \times 10^7 \text{ s}^{-1}$  for 16-PCSL. The results led to the conclusion that the hydrophobic channel has an hourglass-like shape, with the funnel getting narrower around the  $n = 10$  position of the lipid chain, consistent with previously crystallographic structural models (Vetting and Ohlendorf 2000; Ferraroni et al. 2004). In another report, the lipid bound to the enzyme is capable of changing the CCD kinetic profile, from the classic Michaelis–Menten to a cooperative scheme (Mesquita et al. 2013). These results exemplify the relevance of the previous study and give new insights into the CCD regulation upon cyclic hydrocarbon accumulation. More than that, it shows how to study a general interaction between a free lipid and a protein. Such an approach can be extended for any stearic acid, lysophospholipid, acyl-CoA esters and so on, since it is correctly labeled.

## Case 2. Tissue-non-specific alkaline phosphatase (TNAP)

Mammalian alkaline phosphatases (APs) are a class of exoplasmic membrane-bound enzymes that hydrolyze or transphosphorylate a broad range of phosphate compounds at alkaline pH (Harris 1989; McComb et al. 1979). APs are attached to the outer leaflet of the cytoplasmic membrane via a covalent post-translational insertion of a glycosylphosphatidylinositol (GPI) anchor to their carboxyl termini. This allowed them to concentrate on the cell lipid bilayers (Moran et al. 1992; Schreier et al. 1994). Tissue-non-specific alkaline phosphatase (TNAP), one of the three proteins encoded by the four existing human AP genes, is a zinc homodimeric metalloenzyme (Le Du et al. 2001; Sowadski et al. 1985) (Fig. 2), ubiquitously expressed in multiple tissues (Millán 2006). Although the exact physiological roles of TNAP remain unclear, it has been recognized to promote bone and cartilage mineralization (Anderson 1995) by playing a dual role: as an ATPase/ADPase, TNAP generates a pool of inorganic phosphate available for calcification (Ciancaglini et al. 2010); and as a pyrophosphatase, TNAP hydrolyzes inorganic pyrophosphate, a mineralization inhibitor, thus facilitating mineral precipitation and growth (McComb et al. 1979; Moss et al. 1967; Whyte 1994; Rezende et al. 1998).

Lipid composition, membrane curvature, and membrane fluidity have been shown to modulate the catalytic properties of GPI-anchored enzymes (Simão et al. 2010; Sesana et al. 2008; Lehto and Sharom 1998, 2002a). More importantly, lipid membranes, particularly those composed of dipalmitoylphosphatidylcholine (DPPC) and dipalmitoylphosphatidylserine, play a crucial role in the biomineralization process (Simão et al. 2010), which highlights the relevance of studies on TNAP-membrane interactions. Garcia et al. (2015) investigated the unknown effects of membrane-embedded TNAP on the structural organization of DPPC liposomes as model membranes. The authors were interested in addressing two questions: (1) is the GPI anchor indeed and the only responsible for TNAP association to membranes; and (2) what are the changes on the lipid structural dynamics upon TNAP incorporation? To do so, they used phospholipids spin-labeled in the head group region and at positions C5 and C16 of the lipid acyl chain so that the bilayer-to-water interface as well as the center of the hydrophobic core of the membrane could be monitored in protein-free and protein-embedded membranes.

Overall, line shape changes of the ESR spectra of the spin-labeled lipids upon TNAP reconstitution into liposomes indicated a decreased membrane packing and an increased membrane fluidity of all regions monitored (Fig. 3a). The structural organization and fluidity of DPPC bilayers were affected by TNAP in such a way that the membrane orienting potential (order parameter  $S_0$ ; Fig. 3a) and lipid mobility (R, Fig. 3a),

calculated from NLLS spectral simulations, dramatically deviated from those corresponding to the DPPC gel phase, with the most pronounced effect observed in the middle of the lipid bilayer. The rotational diffusion rate of 16-PCSL increased four-fold in the TNAP-reconstituted DPPC proteoliposomes, thus indicating long-reaching modifications of the bilayer. Additionally, the perturbation in the head group region suggested that the protein itself does not directly interact with the lipids. Thus, any disturbance on the bilayer properties due to modifications of membrane surface charge, lipid composition, membrane fluidity, etc., would be transmitted to the protein solely through its GPI anchor (Lehto and Sharom 2002b).

Finally, when treated with phosphatidylinositol phospholipase C (PIPLC), GPI-anchored TNAP-containing proteoliposomes released most of the proteins into solution, causing a decrease in enzyme activity and a negligible effect on the lipid structural dynamics of the membranes. In fact, ESR spectra of DOPTC and 5-PCSL in PIPLC-treated proteoliposomes are very similar to those from TNAP-free DPPC liposomes (Fig. 3b). This means that membrane attachment of TNAP is crucial for enzyme activity and that the GPI-anchored protein as a whole is responsible for the perturbation of the structural organization of the membranes.

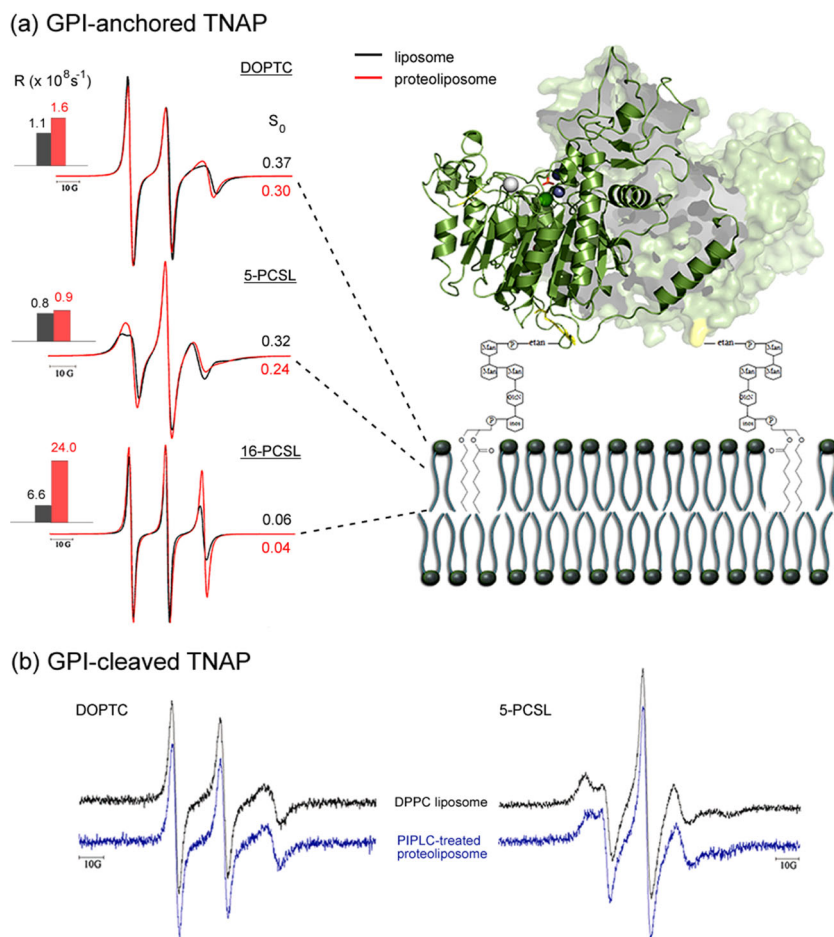
Taken together, the results highlight the relevance of TNAP-lipid interactions in the ordered DPPC gel phase for protein function, since GPI-anchored APs preferentially associate with either an ordered gel phase or lipid-ordered domains of sphingolipid-enriched and cholesterol-enriched lipid rafts (Schroeder et al. 1998; Saslowsky et al. 2002).

## Case 3. Brain fatty acid-binding protein (B-FABP)

FABPs are a group of cytoplasmic molecules that bind, transport, and deliver fatty acids (FA) and other lipids to different sites of utilization (Furuhashi and Hotamisligil 2008; Hertzler and Bernlohr 2000; Lucke et al. 2003). Also called lipid chaperones, they constitute a group of nine different 14- to 15-kDa abundantly expressed intracellular proteins (Glatz and Van der Vusse 1996) that reversibly bind one or two saturated or unsaturated long-chain FAs with high affinity (Coe and Bernlohr 1998; Zimmerman and Veerkamp 2002). The FA binding pocket is located inside a  $\beta$ -barrel (Fig. 1b), a structural motif shared by all nine FABP types (Furuhashi and Hotamisligil 2008; Storch and Thumser 2010; Chmurzynska 2006). Since the interior cavity is solvent-inaccessible, the entry or exit of the substrate requires an as yet unknown protein conformational change. The current hypothesis is that membrane-associated FABPs deliver FAs to membranes through a direct interaction of the *N*-terminal helix–loop–helix ‘cap’ domain (Fig. 1B), a flexible area also known as the ‘portal region’ (Sacchetti et al. 1989).

Dyszy et al. (2013) addressed two questions: (1) is the ‘portal region’ indeed responsible for membrane binding;

**Fig. 3** Relevance of GPI anchor on membrane ordering, dynamics and catalytic properties of TNAP. **a** Left NLLS of ESR spectra of TNAP-free (black) and TNAP-containing (red) spin-labeled DPPC membranes along with the rotational diffusion rates ( $R$ ) and order parameters ( $S_0$ ) obtained from the best fits. Right Hypothetical topology model of the GPI-anchored protein in a lipid bilayer. Protein does not lie on the membrane surface. **b** DOPTC and 5-PCSL ESR spectra obtained in pure DPPC liposomes (black) and after cleavage of the protein GPI anchor from TNAP-reconstituted DPPC proteoliposomes by phosphatidylinositol phospholipase C (PIPLC). Smaller spectral changes are attributed to yet-membrane-associated GPI-anchored TNAP. In the latter case, TNAP enzymatic properties decreased by 70%. Adapted from (Garcia et al. 2015) with permission



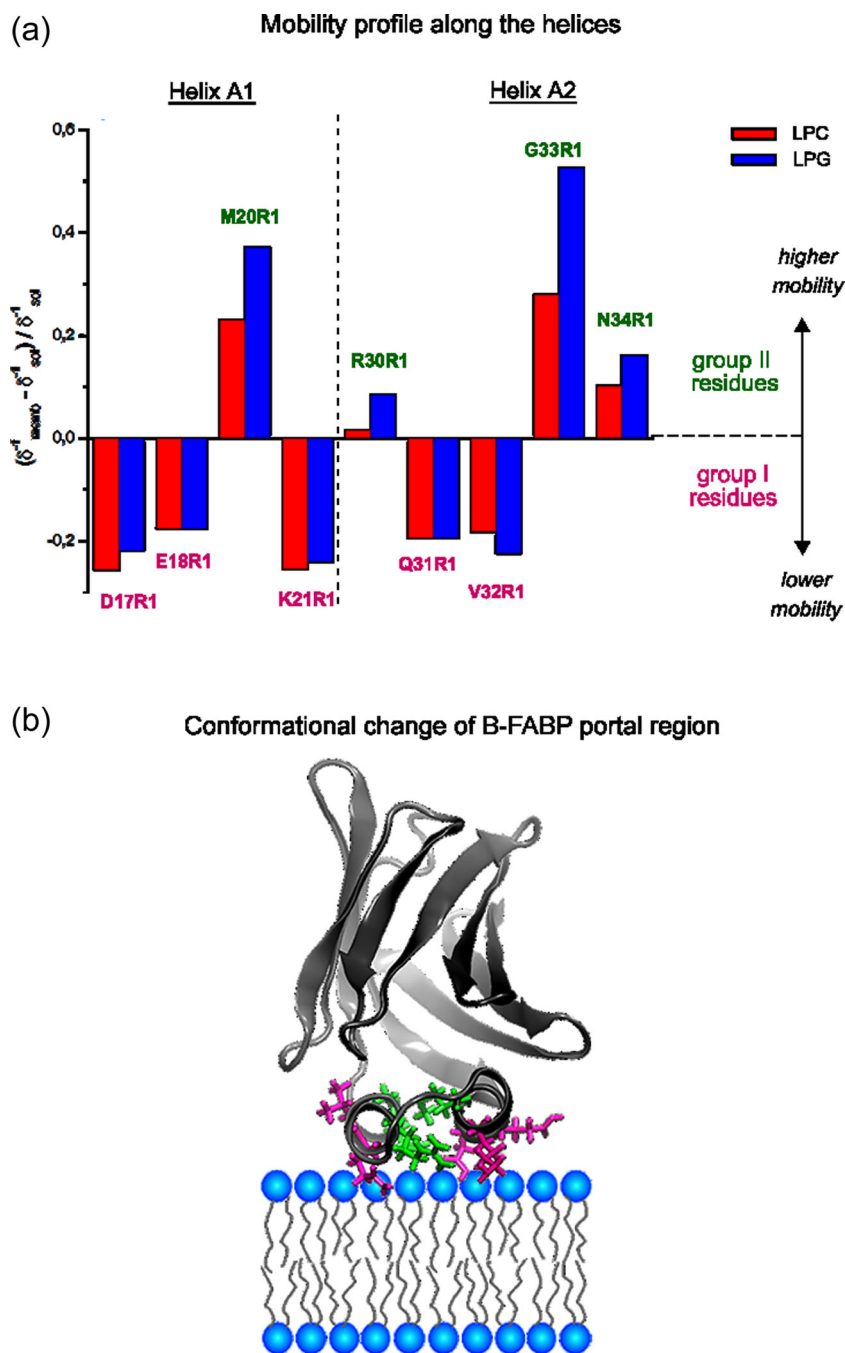
and (2) what are the protein conformational changes that lead to FA delivery into the membrane? To address those questions, the authors engineered nine Cys-mutants along the two helices (four residues in helix A1 and five in helix A2), one at a time, and attached MTSL to those positions. ESR was then used to probe the polarity and mobility changes of each residue upon membrane interaction (Fig. 2b). An almost periodic mobility change of the R1 side chain was found upon membrane binding relative to the protein in solution (Fig. 4a). Interestingly, the residues that presented higher mobility (disordered state) compared to the protein in solution were those whose side chains were oriented in between the two helices (group II, green, Fig. 4b), whereas residues that presented decreased mobility (ordered state) upon membrane interaction were those whose side chains pointed outwards the helices (group I, magenta, Fig. 4b).

Dyszy and coworkers also found that, except for two helix-A2 C-terminal mutants, the local polarity around the nitroxide radical decreased upon micelle interaction for all residues investigated, clearly indicating that the portal region is indeed responsible for membrane binding. Another interesting finding that might possibly be involved in the mechanism of membrane binding and fatty acid delivery was the interplay

between the two spectral components present in the G33R1 and D17R1 ESR spectra. Upon membrane interaction, the more immobilized G33R1 spin population vanishes and the flexible one becomes dominant, whereas a previously non-existent ordered population becomes evident in the D17R1 spectrum (arrow in Fig. 2b). Furthermore, D17R1 and K21R1 presented the most ordering effect (Fig. 4a) and polarity changes upon micelle binding, suggesting that helix A1 stabilizes the protein-membrane complex. Interestingly, due to the charge-dependent polarity changes of G33R1, the helix A2 C-terminus seems to play a unique role in membrane recognition by potentially acting as a sensor of lipid charge. Finally, the authors also highlighted the importance of the whole surface electrostatic potential of the portal region for the mechanism of membrane binding and FA delivery, since point mutations of acidic (Asp17 and Glu18) or basic (Lys21 and Arg30) residues still enable the protein to interact with the biomimetic system, but prevents it to discriminate membrane charge.

Taken together, the SDSL-ESR approach by Dyszy et al. (2013) provided direct evidence for the formation of a transient protein-membrane collisional complex through the interaction of the B-FABP portal region with the membrane.

**Fig. 4** Putative structure–function–dynamics correlation of B-FABP. **a** Changes on the local mobility and polarity profiles of spin-labeled residues along helices A1 and A2 in the presence of LPC (red) or LPG (blue) micelles relative to the protein in solution. The mobility profile was calculated as the difference between the inverse central linewidth ( $\delta^{-1}$ ) of the ESR spectrum of a particular residue in the membrane-bound state and the solution state and normalized to the  $\delta^{-1}$  in the absence of the membrane. Positive values mean higher mobility of the MTSL probe relative to the membrane-unbound state, represented here by group II, green residues, whereas negative values indicate a more ordered state of the membrane-bound protein, represented by the group I, magenta residues. Note that only group II-residues experienced a significant lipid charge-dependent mobility changes, with the great disordering effect observed for G33R1. **b** Hypothetical membrane-docked B-FABP structure illustrating the two group of residues (group I, magenta; group II, green) that experience different conformational changes upon membrane interaction. Both mobility changes and structural rearrangements of helices A1 and A2 might contribute to membrane binding and FA delivery mechanisms. See text for more details. Adapted from (Dyszy et al. 2013) with permission



The results also led the authors to provide a hypothetical model for the putative gating and FA delivery mechanisms of B-FABP: upon binding to the acceptor membrane, the solvent-accessible residues of helices A1 and A2 dock into the membrane and become ordered. This causes a reorientation of the helices so that the residues in between the helices undergo a conformational transition from a packed to a disordered state. The resulting effect is the stabilization of a more opened conformation of the helices that facilitates FA delivery from the protein-binding site to the membrane through the increased free space in between the helices.

#### Case 4. Dihydroorotate dehydrogenases (DHODH)

An elegant example of how ESR experiments from both membrane and protein perspectives can help proposing a particularly important biological mechanism related to protein–membrane interaction is given by the case of the enzyme DHODH in *E. coli* (Couto et al. 2008, 2011). DHODH is responsible for the only redox reaction of the de novo pyrimidine biosynthesis pathway (Bjornberg et al. 1997) in which it catalyzes the oxidation of (S)-dihydroorotate to orotate using flavine as a co-factor (Jones 1980). Since many parasites use only the de



novo pathway to obtain pyrimidines and due to the vital relevance of DHODH to this pathway, this protein has been considered as an excellent target for drug design (Fairbanks et al. 1995; Herrmann et al. 2000). DHODHs are divided into two different families based on sequence similarity, cell localization, and substrate preferences (Bjornberg et al. 1997). *E. coli* DHODH (EcDHODH) is a family-2 member, which means that it is a monomeric membrane-associated protein that uses quinone as a biological oxidant agent (Couto et al. 2008, 2011; Vicente et al. 2015). Family-2 members have an N-terminal extension that folds into two  $\alpha$ -helices and a  $3_{10}$  helix that presumably function as a quinone harbor domain (Fig. 5). To get insights into how EcDHODH fishes quinones out of the membrane, Couto et al. (2008, 2011) performed ESR experiments from both protein and membrane perspectives. Using lipids labeled in the polar head and at positions 5, 10, 12, and 16 of the lipid acyl chain, the authors monitored the effects of EcDHODH on the structural integrity of model membranes upon protein binding. The results indicated that the membrane-associated EcDHODH led to a spacer effect between positions 5 and 10 of the carbon atoms of the lipid bilayer (Couto et al. 2008), strong evidence of a peripheral

docking of the protein in the membrane (Fig. 5a). Couto and colleagues observed two spectral components for 5-PCSL and 10-PCSL (arrows in Fig. 5a), and based on the high values of the isotropic hyperfine splitting (16.0 G) and of the rotational diffusion rate ( $1.47 \times 10^8 \text{ s}^{-1}$ ) for the second spin population, the authors concluded that a defect-like structure was formed by the adhesion of the EcDHODH N-terminal domain into the vesicle (Couto et al. 2008).

To monitor the interaction from the protein perspective, the authors labeled four residues of the EcDHODH N-terminal extension with MTSL (Y2 and F5 from helix 1; H19 and F21 from helix 2 – Fig. 5) (Couto et al. 2011). To obtain information on the ordering and mobility upon membrane interaction, ESR spectra of the nitroxide-labeled protein were recorded with vesicles (Fig. 5b). Overall, changes of the line shape of the spectra clearly indicated protein insertion into the model membrane. NLLS simulations provided higher rotational diffusion rates for helix 1 residues as compared to helix 2 residues, suggesting that helix 1 is more conformationally flexible than helix 2 (Fig. 5b). Additionally, the order parameters for Y2R1 and F5R1 were lower than those for the helix 2 mutants, indicating, in addition, larger amplitude of motion of

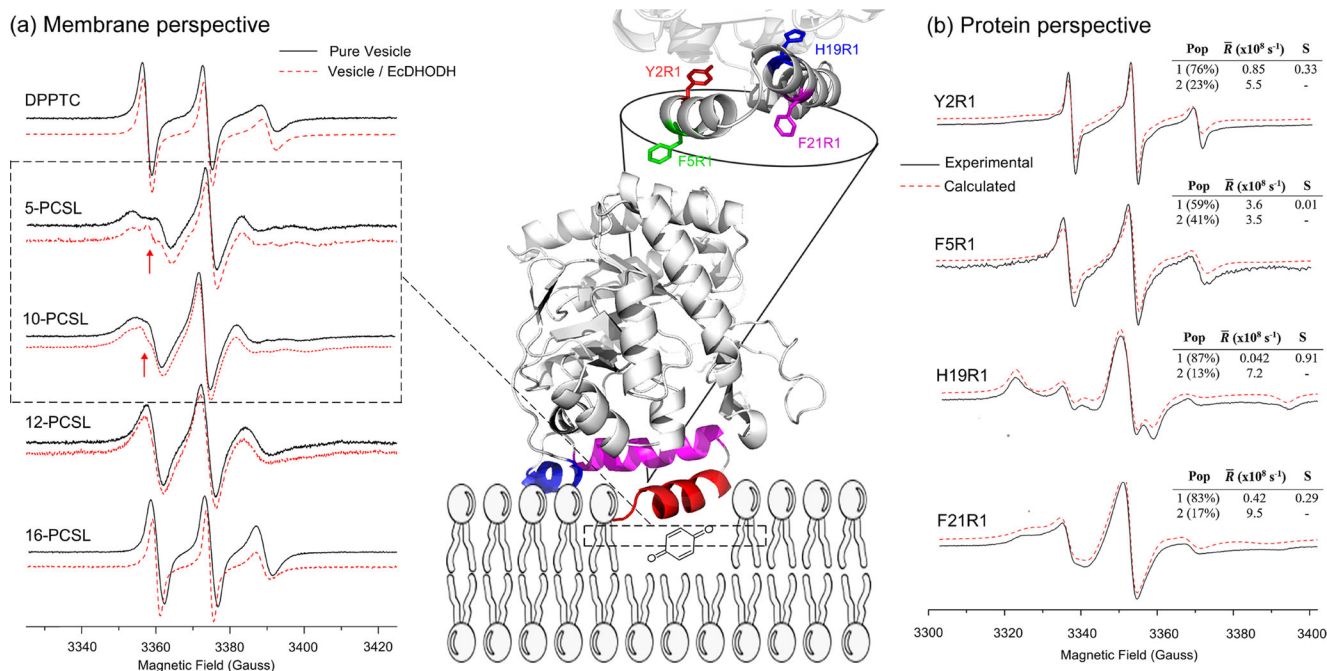


**Fig. 5** Unraveling EcDHODH function from protein and membrane perspectives. *Center* Cartoon representation of EcDHODH (PDB ID: 1F76) attached to a hypothetical bilayer membrane, fishing out the membrane-embedded quinone. The  $\alpha$ -helix 1 (red) is responsible for membrane interaction, the  $\alpha$ -helix 2 (magenta) and the  $3_{10}$  helix (blue) both act like a “rigid base” by which the  $\alpha$ -helix 1 performs the open-to-close mechanism (see the text for more details). At the *top* is shown the protein amino acid positions used for SDSL (Y2 and F5 from  $\alpha$ -helix 1; H19 and F21 from  $\alpha$ -helix 2). **a** *Membrane perspective* ESR spectra of lipids labeled in the head group (DPPTC) and at positions 5, 10, 12, and

16 (*n*-PCSL) of the lipid acyl chain with (red) and without (black) EcDHODH. The narrower component of the two-spectral feature of 5- and 10-PCSL ESR spectra (arrows in the dashed square) reports on the defect-like structure induced by EcDHODH in the lipid bilayer. **b** *Protein perspective* Experimental (solid lines, black) and calculated (dashed lines, red) ESR signals of the single-cysteine EcDHODH mutants labeled with the MTSL probe along with the best-fit rotational diffusion rates ( $R$ ) and order parameters ( $S$ ) obtained from NLLS simulations. The relative population of the two components is also shown. Adapted from (Couto et al. 2008, 2011) with permission

helix 1. Both Y2R1 and F5R1 spectra were fitted with two spectral components associated with the coexistence of two conformationally different populated states possessing different local ordering and dynamics: one flexible and the other in a more rigid conformation (Fig. 5b).

Similar to the previous mutants, ESR spectra of helix 2 mutants H19R1 and F21R1 also showed coexistence of two spectral components. However, different from those, the narrower component, characterized by a very fast motion with no ordering and a very high isotropic hyperfine splitting (16.6 G), was attributed to free spin label in solution. On the other hand, the second component of H19R1 and F21R1 showed a comparatively distinct feature of mobility and order parameters: while the spin probe at position 19 experienced a high ordered environment and a slow motion, the R1 side chain at position 21 experienced a comparatively lower ordering and higher mobility (Fig. 5b). This result indicated a less tightly packed arrangement of helix 2 at position 21 than at position 19 and basically revealed the orientation of their side chains in the protein structure; while the R1 side chain at position 19 makes tertiary contacts to residues of the protein's interior, it points outwards the protein in the F21R1 mutant.

The SDSL-ESR approach by Couto et al. (2011) has undoubtedly shown that helix 2 experiences a more rigid conformation as compared to helix 1, whereas helix 1 residues present two conformational states in the ESR timescale. These results led the authors to conclude that the N-terminal extension of EcDHODH undergoes an open-to-close conformational change that could serve as the molecular mechanism to bring quinones, which are dispersed in the membrane, to the enzyme active site. This is a particularly powerful example of the application of spin labeling ESR to help unraveling a complex biological mechanism by selectively probing their major actors so that they can report on local structural and dynamics changes that might be important to their function.

## Conclusions and perspectives

Many different cell functions rely on transient membrane–protein interaction so it is highly relevant to have tools that shed light on molecular aspects of those interactions. With the development of pulsed ESR methods in the last decade or so, ESR has experienced a renaissance in the field of membrane and protein structural biology, contributing to elucidating important biological functions (McHaourab et al. 2011). Despite that, CW ESR spectroscopy can still successfully bridge structure and dynamics to the mechanism of action of protein–lipid systems. We have presented here a brief review on how spin labelling ESR can be used to obtain local structural and dynamic information on lipid–protein interactions from the perspective of both interacting partners, and how ESR spectral changes provide new insights into different biologically

important phenomena. It is possible to identify differences in molecular dynamics by simply observing changes in the spectral line-shape, a trivial task even for a general user. If a more thorough analysis is necessary, spectral simulations can be performed to assess a group of physicochemical parameters, such as rotational diffusion rates and order parameters. The examples discussed in this review can be used as a guide for sample preparation, data measurement and analyses, thus allowing biologists, biochemists, physicists and biophysicists to employ ESR to tackle problems based on lipid–protein interactions.

**Acknowledgments** The authors acknowledge the University of São Paulo, Fundação de Amparo à Pesquisa do Estado de São Paulo (FAPESP Grants No 2010/17662-8 and 2012/20367-3) and Conselho Nacional de Desenvolvimento Científico e Tecnológico (CNPq) for the financial support. LGMB and LFSM hold FAPESP scholarships (2014/00206-0 and 2012/13309-7).

## Compliance with ethical standards

**Conflict of Interest** Luis G. Mansor Basso declares that he has no conflict of interest.

Luis F. Santos Mendes declares that he has no conflict of interest.

Antonio J. Costa-Filho declares that he has no conflict of interest.

**Ethical approval** This article does not contain any studies with human participants or animals performed by any of the authors.

## References

- Alberts B, Johnson A, Lewis J, Raff M, Roberts K and Walter P (2007) *Molecular biology of the cell* (5th edn). Garland, New York
- Altenbach C, Greenhalgh DA, Khorana HG, Hubbell WL (1994) A collision gradient method to determine the immersion depth of nitroxides in lipid bilayers: application to spin labeled mutants of bacteriorhodopsin. *Proc Natl Acad Sci U S A* 91:1667–1671
- Anderson HC (1995) Molecular biology of matrix vesicles. *Clin Orthop Relat Res* 314:266–280
- Arora A, Tamm LK (2001) Biophysical approaches to membrane protein structure determination. *Curr Opin Struct Biol* 11:540–547
- Atlas RM, Cerniglia CE (1995) Bioremediation of petroleum pollutants — diversity and environmental aspects of hydrocarbon biodegradation. *Bioscience* 45:332–338
- Barroso RP, Basso LGM, Costa-Filho AJ (2015) Interactions of the antimalarial amodiaquine with lipid model membranes. *Chem Phys Lipids* 186:68–78
- Basso LGM, Rodrigues RZ, Naal RMZG, Costa-Filho AJ (2011) Effects of the antimalarial drug primaquine on the dynamic structure of lipid model membranes. *Biochim Biophys Acta* 1808(1):55–64
- Berliner LJ and Reuben J (1989) *Biological magnetic resonance, vol 8: Spin labeling theory and applications* (Berliner LJ, Reuben J, eds). Plenum, New York
- Berliner LJ, Eaton SS, Eaton GR (2000) *Distance measurements in biological systems by EPR*. Plenum, New York
- Bjornberg O, Rowland P, Larsen S, Jensen KF (1997) Active site of dihydroorotate dehydrogenase A from *Lactococcus lactis* investigated by chemical modification and mutagenesis. *Biochemistry* 36:16197–16205

- Borbat PP, Freed JH (1999) Multiple-quantum ESR and distance measurements. *Chem Phys Lett* 313:145–154
- Borbat PP, Costa-Filho AJ, Earle KA, Moscicki JK, Freed JH (2001) Electron spin resonance in studies of membranes and proteins. *Science* 291(5502):266–269
- Brockman H (1999) Lipid monolayers: why use half a membrane to characterize protein-membrane interactions? *Curr Opin Struct Biol* 9(4):438–443
- Budil DE, Lee S, Saxena S, Freed JH (1996) Nonlinear-least-squares analysis of slow-motion EPR spectra in one and two dimensions using a modified Levenberg-Marquardt algorithm. *J Magn Reson* 120:155–189
- Bugg TDH, Ramaswamy S (2008) Non-heme iron-dependent dioxygenases: Unravelling catalytic mechanisms for complex enzymatic oxidations. *Curr Opin Chem Biol* 12:134–140
- Cañadas O, Casals C (2013) Differential scanning calorimetry of protein-lipid interactions. *Methods Mol Biol* 974:55–71
- Chmurzynska A (2006) The multigene family of fatty acid-binding proteins (FABPs): function, structure and polymorphism. *J Appl Genet* 47:39–48
- Cho W, Stahelin RV (2005) Membrane-protein interactions in cell signaling and membrane trafficking". *Annu Rev Biophys Biomol Struct* 34:119–151
- Ciancaglini P, Yadav MC, Simão AM, Narisawa S, Pizauro JM, Farquharson C, Hoylaerts MF, Millán JL (2010) Kinetic analysis of substrate utilization by native and TNAP-, NPP1-, or PHOSPHO1-deficient matrix vesicles. *J Bone Miner Res* 25(4):716–723
- Citadini APS, Pinto APA, Araujo APU, Nascimento OR, Costa-Filho AJ (2005) EPR studies of corocatechol 1,2-dioxygenase: Evidences of iron reduction during catalysis and of the binding of amphipatic molecules. *Biophys J* 88:3502–3508
- Coe NR, Bernlohr DA (1998) Physiological properties and functions of intracellular fatty acid-binding proteins. *Biochim Biophys Acta* 1391:287–306
- Columbus L, Hubbell WL (2002) A new spin on protein dynamics. *Trends Biochem Sci* 27:288–295
- Costa-Filho AJ, Borbat PP, Crepeau RH, Ge M, Freed JH (2003) Lipid-gramicidin interactions: Dynamic structure of the boundary lipid by 2D-ELDOR. *Biophys J* 84:3364–3378
- Couto SG, Nonato MC, Costa-Filho AJ (2008) Defects in Vesicle Core Induced by *Escherichia coli* Dihydroorotate Dehydrogenase. *Biophys J* 94:1746–1753
- Couto SG, Nonato MC, Costa-Filho AJ (2011) Site directed spin labeling studies of *Escherichia coli* dihydroorotate dehydrogenase N-terminal extension. *Biochem Biophys Res Commun* 414:487–492
- Dua X, Hladya V, Britt D (2005) Langmuir monolayer approaches to protein recognition through molecular imprinting. *Biosens Bioelectron* 20(10):2053–2060
- Dyszy F, Pinto AP, Araújo AP, Costa-Filho AJ, 3 (2013) Probing the interaction of brain fatty acid binding protein (B-FABP) with model membranes. *PLoS ONE* 8:e 60198
- Fairbanks LD, Bofill M, Ruckemann K, Simmonds HA (1995) Importance of ribonucleotide availability to proliferating Tlymphocytes from healthy humans. Disproportionate expansion of pyrimidine pools and contrasting effects of de novo synthesis inhibitors. *J Biol Chem* 270:29682–29689
- Fajer PG (2000) Electron spin resonance spectroscopy labeling in peptide and protein analysis. In Meyers RA (ed). *Encyclopedia of analytical chemistry*, Wiley, Chichester, pp 5725–5761
- Ferraroni M, Solyanikova IP, Kolomytseva MP, Scozzafava A, Golovleva L, Briganti F (2004) Crystal structure of 4-chlorocatechol 1,2-dioxygenase from the chlorophenol-utilizing Gram-positive *Rhodococcus opacus* 1CP. *J Biol Chem* 279:27646–27655
- Franks WT, Linden AH, Kunert B, van Rossum BJ, Oschkinat H (2012) Solid-state magic-angle spinning NMR of membrane proteins and protein-ligand interactions. *Eur J Cell Biol* 91:340–348
- Furuhashi M, Hotamisligil GS (2008) Fatty acid-binding proteins: role in metabolic diseases and potential as drug targets. *Nat Rev Drug Discov* 7(6):489–503
- Garcia AF, Lopes JLS, Costa-Filho AJ, Wallace BA, Araujo APU (2013) Membrane interactions of S100A12 (Calgranulin C). *PLoS ONE* 8(12), e8255
- Garcia AF, Simão AM, Bolean M, Hoylaerts MF, Millán JL, Ciancaglini P, Costa-Filho AJ (2015) Effects of GPI-anchored TNAP on the dynamic structure of model membranes. *Phys Chem Chem Phys* 17(39):26295–26301
- Ge M, Freed JH (1998) Polarity profiles in oriented and dispersed phosphatidylcholine bilayers are different: an electron spin resonance study. *Biophys J* 74:910–917
- Ge M, Freed JH (2009) Fusion peptide from influenza hemagglutinin increases membrane surface order: An electron-spin resonance study. *Biophys J* 96(12):4925–4934
- Glatz JFC, Van der Vusse GJ (1996) Cellular fatty acid-binding proteins: their function and physiological significance. *Prog Lipid Res* 35:243–282
- Goñi F (2002) Non-permanent proteins in membranes: When proteins come as visitors (Review). *Mol Membr Biol* 19(4):237–245
- Guzzi R, Bartucci R (2015) Electron spin resonance of spin-labeled lipid assemblies and proteins. *Arch Biochem Biophys* 580:102–111
- Hanson GR, Berliner LJ (2009) High resolution EPR: applications to metalloenzymes and metals in medicine, *Biological Magnetic Resonance*. 2009th Edition. Springer, New York [N.Y.]
- Harris H (1989) The human alkaline phosphatases: what we know and what we don't know. *Clin Chim Acta* 186:133–150
- Hemminga MA (2007) Introduction and future of site-directed spin labeling of membrane proteins. In: Hemminga MA, Berliner LJ (eds) *ESR spectroscopy in membrane biophysics*. *Biological magnetic resonance*, vol 27. Springer, Berlin, pp 1–16
- Herrmann ML, Schleyerbach R, Kirschbaum BJ (2000) An immunomodulatory drug for the treatment of rheumatoid arthritis and other autoimmune diseases. *Immunopharmacology* 47:273–289
- Hertz AV, Bernlohr DA (2000) The mammalian fatty acid binding protein multigene family: Molecular and genetic insights into function. *Trends Endocrinol Metab* 11:175–180
- Hubbell WL, Altenbach C (1994) Investigation of structure and dynamics in membrane proteins using site-directed spin labeling. *Curr Opin Struct Biol* 4(4):566–573
- Hubbell WL, McConnell HM (1969) Orientation and motion of amphiphilic spin labels in membranes. *Proc Natl Acad Sci U S A* 64:20–27
- Hubbell WL, McConnell HM (1971) Molecular motions in spin-labeled phospholipids and membranes. *J Am Chem Soc* 93:314–326
- Hubbell WL, Gross A, Langen R, Lietzow MA (1998) Recent advances in site-directed spin labeling of proteins. *Curr Opin Struct Biol* 8:649–656
- Hubbell WL, Cafiso DS, Altenbach C, 9 (2000) Identifying conformational changes with site-directed spin labeling. *Nat Struct Biol* 7:735–739. 98: 7777–7782
- Hubbell WL, Lopez CJ, Altenbach C, Yang Z (2013) Technological advances in site-directed spin-labeling of proteins. *Curr Opin Struct Biol* 23:725–733
- Humphrey W, Dalke A, Schulten K (1996) VMD - Visual Molecular Dynamics. *J Molec Graph* 14:33–38
- Hurley JH (2006) Membrane binding domains. *Biochim Biophys Acta* 1761:805–811
- Jeschke G (2012) DEER distance measurements on proteins. *Annu Rev Phys Chem* 63:419–446
- Jeschke G, Polyhach Y (2007) Distance measurements on spin-labelled biomacromolecules by pulsed electron paramagnetic resonance. *Phys Chem Chem Phys* 9:1895–1910

- Jeschke G, Bender A, Paulsen H, Zimmermann H, Godt A (2004) Sensitivity enhancement in pulse EPR distance measurement. *J Magn Reson* 169:1–12
- Jo S, Kim T, Iyer VG, Im W (2008) CHARMM-GUI: A Web-based Graphical User Interface for CHARMM. *J Comput Chem* 29:1859–1865
- Johnson AE (2005) Fluorescence approaches for determining protein conformations, interactions and mechanisms at membranes. *Traffic* 6(12):1078–1092
- Jones ME (1980) Pyrimidine nucleotide biosynthesis in animals: genes, enzymes, and regulation of UMP biosynthesis. *Annu Rev Biochem* 49:253–279
- Judge PJ, Taylor GF, Dannatt HR, Watts A (2015) Solid-state nuclear magnetic resonance spectroscopy for membrane protein structure determination. *Method Mol Biol* 126:331–47
- Kleinschmidt JH (2013) Lipid–protein interactions. *Methods and protocols*. Springer, Berlin
- Langen R, Oh KJ, Cascio D, Hubbell WL (2000) Crystal structures of spin labeled T4 lysozyme mutants: implications for the interpretation of EPR spectra in terms of structure. *Biochemistry* 39:8396–8405
- Le Du MH, Stigbrand T, Taussig MJ, Ménez A, Stura EA (2001) Crystal structure of alkaline phosphatase from human placenta at 1.8 Å resolution. *J Biol Chem* 276:9158–9165
- Lehto MT, Sharom FJ (1998) Release of the glycosylphosphatidylinositol-anchored enzyme ecto-5'-nucleotidase by phospholipase C: catalytic activation and modulation by the lipid bilayer. *Biochem J* 332(Pt 1):101–109
- Lehto MT, Sharom FJ (2002a) Proximity of the protein moiety of a GPI-anchored protein to the membrane surface: a FRET study. *Biochemistry* 41(26):8368–8376
- Lehto MT, Sharom FJ (2002b) PI-specific phospholipase C cleavage of a reconstituted GPI-anchored protein: modulation by the lipid bilayer. *Biochemistry* 41(4):1398–1408
- Lucke C, Gutierrez-Gonzales LH, Hamilton JA (2003) Intracellular lipid binding proteins: evolution, structure, and ligand binding. In: Duttaroy AK, Spener F (eds) *Cellular proteins and their ligand fatty acids—emerging roles in gene expression, health and disease*. Wiley, New York, pp 95–114
- Marsh D (2001) Polarity and permeation profiles in lipid membranes. *Proc Natl Acad Sci U S A* 98:7777–7782
- Marsh D (2008) Protein modulation of lipids, and vice-versa, in membranes. *Biochim Biophys Acta* 1778(7–8):1545–1575
- Marsh D, Watts A (1982) Spin labeling and lipid-protein interactions in membranes. In: Griffith H (ed) *Lipid-Protein Interactions*. Vol. 2. P. C. Jost and O. Wiley-Interscience, New York, pp 53–126
- Marsh D, Watts A, Pates RD, Uhl R, Knowles PF, Esmann M (1982) ESR spin-label studies of lipid-protein interactions in membranes. *Biophys J* 37:265–274
- Matsuo K, Maki Y, Namatame H, Taniguchi M, Gekko K (2016) Conformation of membrane-bound proteins revealed by vacuum-ultraviolet circular-dichroism and linear-dichroism spectroscopy. *Proteins* 84(3):349–359
- McComb RB, Bowers GN, Posen S (1979) *Alkaline phosphatase*. Plenum, New York
- Mchaourab HS, Lietzow MA, Hideg K, Hubbell WL (1996) Motion of spin-labeled side chains in T4 lysozyme. correlation with protein structure and dynamics. *Biochemistry* 35:7692–7704
- McHaourab HS, Steed PR, Kazmier K (2011) Toward the fourth dimension of membrane protein structure: insight into dynamics from spin-labeling EPR spectroscopy. *Structure* 19(11):1549–1561
- Mesquita NCMR, Dyszy FH, Kumagai PS, Araujo APU, Costa-Filho AJ (2013) Amphipatic molecules affect the kinetic profile of *Pseudomonas putida* chlorocatechol 1,2-dioxygenase. *Eur Biophys J* 42:655–660
- Millán JL (2006) *Mammalian alkaline phosphatases: from biology to applications in medicine and biotechnology*. Wiley-VCH, Weinheim
- Moran P, Beasley H, Gorrell A, Martin E, Gribling P, Fuchs H, Gillett N, Burton LE, Caras IW (1992) Human recombinant soluble decay accelerating factor inhibits complement activation in vitro and in vivo. *J Immunol* 149:1736–1743
- Moss DW, Eaton RH, Smith JK, Whitby LG (1967) Association of inorganic-pyrophosphatase activity with human alkaline-phosphatase preparations. *Biochem J* 102:53–57
- Munishkina LA, Fink AL (2007) Fluorescence as a method to reveal structures and membrane-interactions of amyloidogenic proteins. *Biochim Biophys Acta* 1768(8):1862–1885
- Ornston LN, Stanier RY (1966) Conversion of catechol and protocatechuate to beta-ketoadipate by *Pseudomonas putida*. *J Biol Chem* 241:3776–3786
- Páli T, Kóta Z (2013) Studying lipid-protein interactions with electron paramagnetic resonance spectroscopy of spin-labeled lipids. *Methods Mol Biol* 974:297–328
- Redfield A (1965) *The Theory of Relaxation Processes*. *Adv Magn Reson* 1:1
- Rezende LA, Ciancaglini P, Pizauro JM, Leone FA (1998) Inorganic pyrophosphate-phosphohydrolytic activity associated with rat osseous plate alkaline phosphatase. *Cell Mol Biol* 44:293–302
- Sacchettini JC, Gordon JI, Banaszak LJ (1989) Crystal structure of rat intestinal fatty-acid-binding protein—refinement and analysis of the *Escherichia coli*-derived protein with bound palmitate. *J Mol Biol* 208:327–339
- Sahu ID, Lorigan GA (2015) Biophysical EPR studies applied to membrane proteins. *J Phys Chem Biophys* 5(6):188
- Saliba AE, Vonkova I, Gavin AC (2015) The systematic analysis of protein–lipid interactions comes of age. *Nat Rev Mol Cell Biol* 16(12):73–761
- Saslowsky DE, Lawrence J, Ren X, Brown DA, Henderson RM, Edwardson JM (2002) Placental alkaline phosphatase is efficiently targeted to rafts in supported lipid bilayers. *J Biol Chem* 277(30):26966–26970
- Schneider DJ and Freed JH (1989) Calculating slow motional magnetic resonance spectra. In: Berliner LJ, Reuben J (eds) *Spin labeling theory and applications*, Plenum, New York, pp 1–76
- Schreier H, Moran P, Caras IW (1994) Targeting of liposomes to cells expressing CD4 using glycosylphosphatidylinositol-anchored gp120. Influence of liposome composition on intracellular trafficking. *J Biol Chem* 269:9090–9098
- Schroeder RJ, Ahmed SN, Zhu Y, London E, Brown DA (1998) Cholesterol and sphingolipid enhance the Triton X-100 insolubility of glycosylphosphatidylinositol-anchored proteins by promoting the formation of detergent-insoluble ordered membrane domains. *J Biol Chem* 273(2):1150–1157
- Seelig J, Hasselbach W (1971) A spin label study of sarcoplasmic vesicles. *Eur J Biochem* 21:17–21
- Sesana S, Re F, Bulbarelli A, Salerno D, Cazzaniga E, Masserini M (2008) Membrane features and activity of GPI-anchored enzymes: alkaline phosphatase reconstituted in model membranes. *Biochemistry* 47(19):5433–5440
- Simão AM, Yadav MC, Narisawa S, Bolean M, Pizauro JM, Hoylaerts MF, Ciancaglini P, Millán JL (2010) Proteoliposomes harboring alkaline phosphatase and nucleotide pyrophosphatase as matrix vesicle biomimetics. *J Biol Chem* 285(10):7598–7609
- Situ AJ, Schmidt T, Mazumder P, Ulmer TS (2014) Characterization of membrane protein interactions by isothermal titration calorimetry. *J Mol Biol* 426(21):3670–3680
- Smimova TI, Smimov AI (2015) Peptide-membrane interactions by spin-labeling EPR. *Methods Enzymol* 564:219–258
- Smith WL, Garavito RM, Ferguson-Miller S (2001) Membrane protein structural biology. *Minireview Series J Biol Chem* 276:32393–32394

- Solomon EI, Brunold TC, Davis MI, Kemsley JN, Lee SK, Lehnert N, Neese F, Skulan AJ, Yang YS, Zhou J (2000) Geometric and electronic structure/function correlations in non-heme iron enzymes. *Chem Rev* 100:235–349
- Sowa GZ, Qin PZ (2008) Site-directed spin labeling studies on nucleic acid structure and dynamics. *Prog Nucleic Acid Res Mol Biol* 82: 147–197
- Sowadski JM, Handschumacher MD, Murthy HMK, Foster BA, Wyckoff HW (1985) Refined structure of alkaline phosphatase from *Escherichia coli* at 2.8 Å resolution. *J Mol Biol* 186:417–433
- Storch J, Thumser AE (2010) Tissue-specific functions in the fatty acid-binding protein family. *J Biol Chem* 285:32679–32683
- Stott JB, Povstyan OV, Carr G, Barrese V, Greenwood IA (2015) G-protein  $\beta\gamma$  subunits are positive regulators of Kv7.4 and native vascular Kv7 channel activity. *Proc Natl Acad Sci U S A* 112(20): 6497–6502
- Swamy MJ, Ciani L, Ge M, Smith AK, Holowka D, Baird B, Freed JH (2006) Coexisting domains in the Plasma membranes of live cells characterized by spin-label ESR spectroscopy. *Biophys J* 90:4452–4465
- Tatulian SA (2013) Structural characterization of membrane proteins and peptides by FTIR and ATR-FTIR spectroscopy. *Methods Mol Biol* 974:177–218
- Vauquelin G, Packeu A (2009) Ligands, their receptors and ... plasma membranes. *Mol Cell Endocrinol* 311(1–2):1–10
- Vetting MW, Ohlendorf DH (2000) The 1.8 Å crystal structure of catechol 1,2-dioxygenase reveals a novel hydrophobic helical zipper as a subunit linker. *Structure* 8:429–440
- Vicente EF, Basso LGM, Cespedes GF, Lorenzón EN, Castro MS, Mendens-Giannini MJS, Costa-Filho AJ, Cilli EM (2013) Dynamics and Conformational Studies of TOAC Spin Labeled Analogues of Ctx(Ile21)-Ha Peptide from *Hypsiboas albopunctatus*. *PLoS ONE* 8, e60818
- Vicente EF, Nobre-Pavinatto TM, Pavinatto FJ, Oliveira-Junior ON, Costa-Filho AJ, Cilli EM (2015) N-Terminal Microdomain Peptide from Human Dihydroorotate Dehydrogenase: Structure and Model Membrane Interactions. *Protein Pept Lett* 22:119–129
- Whyte MP (1994) Hypophosphatasia and the role of alkaline phosphatase in skeletal mineralization. *Endocr Rev* 15:439–461
- Wolfs JA, Horváth LI, Marsh D, Watts A, Hemminga MA (1989) Spin-label ESR of bacteriophage M13 coat protein in mixed lipid bilayers. Characterization of molecular selectivity of charged phospholipids for the bacteriophage M13 coat protein in lipid bilayers. *Biochemistry* 28(26):9995–10001
- Wu EL, Cheng X, Jo S, Rui H, Song KC, Dávila-Contreras EM, Qi Y, Lee J, Monje-Galvan V, Venable RM, Klauda JB, Im W (2014) CHARMM-GUI membrane builder toward realistic biological membrane simulations. *J Comput Chem* 35:1997–2004
- Zimmerman AW, Veerkamp JH (2002) New insights into the structure and function of fatty acid-binding proteins. *Cell Mol Life Sci* 59: 1096–1116